LBL-15124
Preprint c.2

Lawrence Berkeley Laboratory
UNIVERSITY OF CALIFORNIA

Materials & Molecular Research Division

RECEIVED
LAWRENCE
BERKELEY LABORATORY
DEC 7 1982
LIBRARY AND
DOCUMENTS SECTION

Submitted to Journal of Nuclear Materials

RAPID HEATING AND VAPORIZATION OF BINARY SOLIDS BY ABSORBING RADIATION - I NUMERICAL MODELING OF HEAT AND MASS TRANSPORT

Chuen-horng Tsai and Donald R. Olander

October 1982

TWO-WEEK LOAN COPY

This is a Library Circulating Copy which may be borrowed for two weeks. For a personal retention copy, call Tech. Info. Division, Ext. 6782.

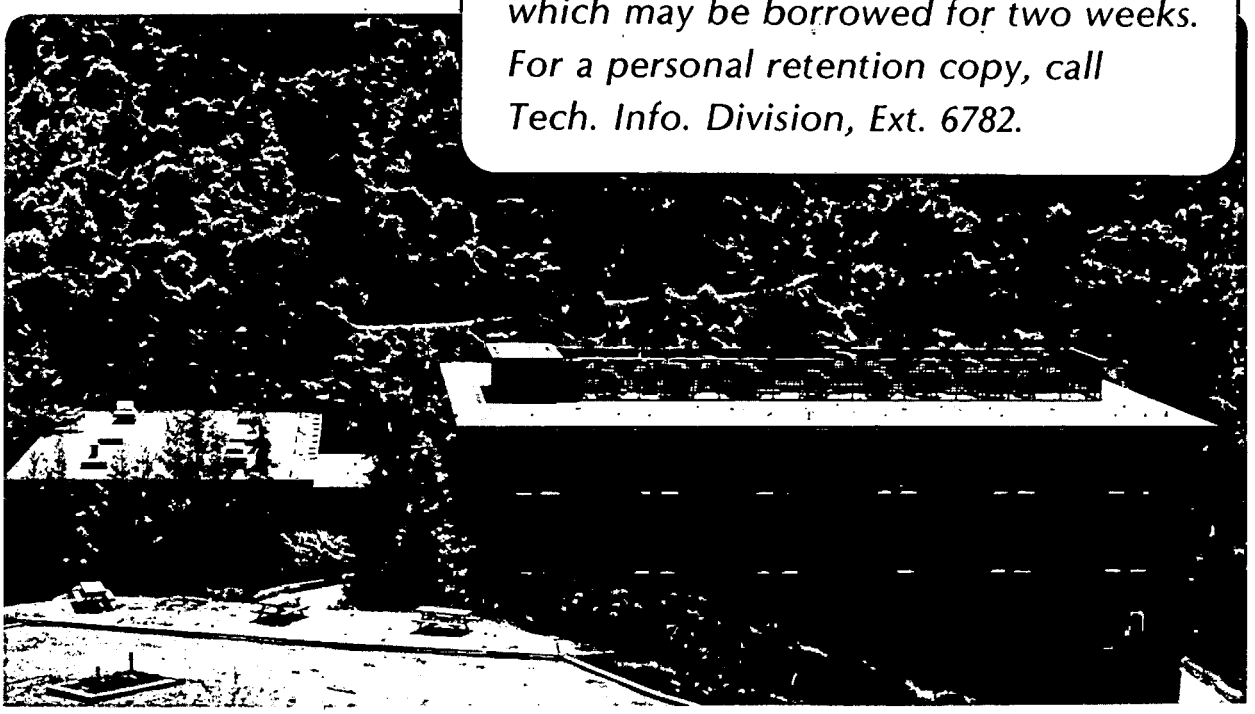

LBL-15124 c.2

Prepared for the U.S. Department of Energy under Contract DE-AC03-76SF00098

DISCLAIMER

This document was prepared as an account of work sponsored by the United States Government. While this document is believed to contain correct information, neither the United States Government nor any agency thereof, nor the Regents of the University of California, nor any of their employees, makes any warranty, express or implied, or assumes any legal responsibility for the accuracy, completeness, or usefulness of any information, apparatus, product, or process disclosed, or represents that its use would not infringe privately owned rights. Reference herein to any specific commercial product, process, or service by its trade name, trademark, manufacturer, or otherwise, does not necessarily constitute or imply its endorsement, recommendation, or favoring by the United States Government or any agency thereof, or the Regents of the University of California. The views and opinions of authors expressed herein do not necessarily state or reflect those of the United States Government or any agency thereof or the Regents of the University of California.

LBL-15124

Rapid Heating and Vaporization of Binary Solids by Absorbing Radiation - I Numerical Modeling of Heat and Mass Transport

Chuen-horng Tsai* and Donald R. Olander

Department of Nuclear Engineering

University of California

and

Materials and Molecular Research Division

Lawrence Berkeley Laboratory

Berkeley, CA 94720 U. S. A.

---

*Present address:

Department of Nuclear Engineering

National Tsing Hua University

Hsinchu, Taiwan

REPUBLIC OF CHINA

This work was supported by the Director, Office of Energy Research, Office of Basic Energy Sciences, Materials Sciences Division of the U.S. Department of Energy under contract #DE-AC03-76SF00098.

ABSTRACT

Pulsed surface irradiation of an absorbing material induces a temperature transient which leads to melting and vaporization. If the target is a two-component solid that evaporates incongruently, the near-surface composition is also perturbed. A mathematical model and numerical solution scheme have been developed to simulate the heat and mass transport processes which result from rapid energy deposition in the surface of a binary solid. The response surface method was used to determine the loss of precision in such a computation due to uncertainties in the material properties at high temperatures.

Application of the method to incongruently-vaporizing UO_2 irradiated by a pulsed laser demonstrated the extent of oxygen depletion of the surface and revealed the sensitivity of the computed temperatures and vaporization rates arising from lack of knowledge of the diffusivity of oxygen in liquid UO_2.

I INTRODUCTION

When an intense pulse of radiation is incident on a highly absorbing solid material, the resulting rise in surface temperature and the generation of temperature gradients beneath the surface produce a variety of physical effects, which include surface vaporization, melting, thermal radiation, thermal stresses, and shock waves. Typical characteristic pulse times (microseconds or greater) are far longer than the time for transfer of the absorbed energy to lattice phonons (picoseconds), so that redistribution of the absorbed energy can be treated as a macroscopic heat conduction process.

In addition, composition redistribution due to incongruent evaporation must be considered if the target material is a compound. In the uranium-oxygen system, for example, oxygen is the preferentially-vaporizing component, and as a result of the limited mobility of oxygen in urania, a deficiency of oxygen develops near the surface. The solid responds to this change in surface composition by diffusion of oxygen from the bulk, thereby creating a concentration distribution in the same near-surface layer which contains the temperature nonuniformity.

Although transient heating has been widely applied to investigate the thermophysical properties of liquid UO_2(1-4), there has been no report of a calculation of the thermal and composition evolution of UO_2 subjected to a single intense surface heat pulse. In their laser pulsing experiments, Ohse et al(2) relied mainly on pyrometric measurement of surface temperatures; their only sub-surface temperature profile calculation(5) was based on a model of Dabby and Paek(6), which assumes a prior(known) steady state surface temperature. Surface oxygen depletion, which cannot be experimentally

determined, was not treated theoretically. The KfK group initially relied on a gasdynamic model to infer vapor temperatures in laser pulsing of UO_2(3) but later switched to pyrometric measurement of the surface temperature(7). Although the solid temperature was not treated theoretically, surface oxygen depletion was calculated from Breitung's "forced congruent evaporation" model(8). This calculation assumes i) a constant, steady state temperature throughout the solid achieved after a step change from low temperature and ii) sufficient time for oxygen diffusion in the solid to establish a steady state O/U distribution in the vicinity of the evaporating surface. Although these restrictions are adequate for the KfK apparatus, they cannot be applied to transient heating pulse of arbitrary temporal shape, particularly when the characteristic time for mass diffusion is of the same order as that of the temperature rise. In such cases, the asymptotic stationary congruent evaporation condition is not achieved.

In the present study, the response of two-component solids to rapid addition of heat at or just beneath the surface of a semi-infinite medium is analyzed by application of appropriate conservation equations and flux laws. Because of the small penetration depth of the temperature and composition perturbations, a one-dimensional analysis of a semi-infinite medium is adequate. The moving boundary effect due to surface ablation, temperature-dependent physical properties and sub-surface melting are taken into account. No radial liquid movement is permitted in the calculation but a planar melting front moves away from the surface. The thermal effect of melting is treated implicitly via the heat capacity term in the bulk. Both penetrating incident radiation, which produces near-surface volumetric heating, and direct surface heating of

opaque solids are allowed. This option is designed not only to accommodate different optical properties of the materials subject to the surface radiation, but also permits application of the calculation to a variety of heat sources such as laser light, electron beam bombardment, energetic ion impingement, and neutron and gamma ray pulse heating. Such transient heating schemes have been proposed for the acquisition of thermochemical data on refractory materials and are often good simulations of the thermal loading on the walls of pulsed thermonuclear fusion reactors.

In one-component or congruently vaporizing multicomponent solids, no composition redistribution occurs and only transport of heat need be considered. In incongruently vaporizing binary solids, recession of the surface is controlled by the rate of evaporation of the less volatile species, but the rate of supply of components to the surface from the interior may be governed by either species. In the zirconium-hydrogen system treated by Olstad and Olander(9), hydrogen diffuses through a rigid zirconium lattice, but because zirconium is nonvolatile, surface recession does not occur. In initially stoichiometric urania, oxygen is the most volatile element because of the high vapor pressure of UO_3 compared to UO. Oxygen is also the more mobile element, and so controls the O/U distribution. In uranium carbide, on the other hand, the metal volatilizes preferentially and leaves behind a carbon-rich solid. However, carbon is more mobile than uranium in the solid and thus controls the composition changes.

Vaporization of the surface affects the temperature and composition in the solid in the following ways. First, the evaporation process con-

stitutes a heat sink at the surface which must be incorporated into the thermal boundary condition. In the limit of very intense heating, all of the incident energy may be utilized in supplying the heat of vaporization, thus limiting the maximum temperature achievable. Second, the recession of the surface caused by ablation produces a moving-boundary complication in the heat transfer analysis. Third, incongruent vaporization causes an imbalance in composition between the surface and the bulk, which generates a diffusive transport of the constituents of the solid near the surface. To treat surface vaporization, it is essential to be able to relate the rate of evaporation to the temperature and composition of the surface. Vaporization of species i due to surface heating is described by the Hertz-Langmiur formula:

$$\Phi_i = \frac{\alpha_i P_i}{\sqrt{2\pi M_i R T_s}} (1 - \beta) \qquad (1)$$

where Φ_i is the molar vaporization flux and P_i is the equilibrium pressure of vapor species i over a condensed phase at the instantaneous temperature T_s and the composition of the ablating surface. M_i is the molecular weight of species i, R is the gas constant, and α_i is the vaporization coefficient.

The vaporization coefficient in Eq(1) contains all of the kinetic restrictions to vaporization arising from molecular processes which occur on the surface before a particle is emitted to the vapor phase. For the surfaces of single crystals of substances which must assemble many atoms into a complex molecule prior to evaporation, α can be considerably less than unity. However, for vaporization of monatomic solids to a monatomic vapor or of solids in which only a modest rearrangement of atoms to form the

vapor molecule is required, α is invariably close to unity(10, 11). For the polycrystalline surfaces of interest here, the evaporation coefficients are larger than for single crystal surfaces. Thus for the examples cited in the previous section, unit evaporation coefficient for steady state vacuum vaporization is probably a very good assumption. In the following analysis, the assumption $\alpha_i = 1$ is retained even for rapid transient heating.

Despite reservations concerning use of Eq(1) expressed by Breitung(4), there is no other known theory for connecting vaporization rates to equilibrium vapor pressures. This formula has been widely applied in steady state vacuum evaporation, being the only means of measuring the vapor pressures of refractory substances such as tungsten. However, the validity of the Hertz-Langmiur formula in rapid transients is a legitimate subject of concern, especially since evaporation rates may be so large that the vapor plume is better described by continuum fluid mechanics than by free molecule flow theory. The gas kinetic theory models of Anisimov(12) and Ytrehus(13) predict collision-dominated flow after a nonequilibrium layer a few mean free paths thick. This theory is based on the assumption that molecules leave the surface with a Maxwell-Boltzmann velocity distribution characteristic of the surface temperature. In integral form, this assumption gives the Hertz-Langmiur formula. Backscattering of emitted particles from the vapor cloud above the surface reduces the vaporization rate by a factor of only $\sim$ 18%, which is the value of the factor β in Eq(1).

Ablation analyses of fusion reactor first walls such as that reported in Ref. 14 use the non-equilibrium vaporization model proposed some time ago by Schrage(15):

$$\Phi_i = \frac{\alpha_i P_i}{\sqrt{2\pi M_i R T_s}} - \frac{\Gamma\, \alpha_i' P_i'}{\sqrt{2\pi M_i R T'}} \qquad (1a)$$

where α_i' is the condensation coefficient (the fraction of molecules impinging on the surface which are not reflected directly back to the gas) and Γ is a bulk flow correction factor. The vapor properties P_i' and T' refer to the continuum fluid which exists outside of the nonequilibrium layer adjacent to the surface.

The factor β in Eq(1) and the second term on the right hand side of Eq(1a) are corrections to the Hertz-Langmiur vacuum evaporation rate due to molecules returning to the surface from the vapor cloud. The choice of Eq(1) or (1a) has a profound effect on the theoretical analysis of surface ablation. If Eq(1a) is employed, the thermal analysis of the condensed phase is coupled to the fluid transport process occuring far from the surface, solely because the vapor temperature and pressure appear in the last term of this formula. The use of Eq(1) to represent nonequilibrium vaporization has two distinct advantages. First, this formula is based on a more thorough treatment of the physics of the vaporization process than is the Schrage model, the shortcomings of which are discussed by Ytrehus(13). Second, the backscattering coefficient β is independent of the state of the vapor immediately adjacent to the surface. This factor depends only on the ratio of the equilibrium vapor pressure of the condensed phase to the pre-pulse background gas pressure. If this ratio is greater than ~ 5, then $\beta = 0.18$ and is independent of all conditions of the blowoff. This backscattering factor applies to steady evaporation. The time to achieve this value has been estimated by Anisimov and Rakhmatulina (16) to be ~ 20 molecular collision times. The latter is approximately the reciprocal of six times the product of the scattering cross section of the evaporating molecules ($\sim 10^{-15}$ cm^2), the density

of the vapor in front of the surface (equal to 2×10^{18} cm^{-3} for a vapor at 1 atm pressure and 4000 K), and the mean molecular speed ($\sim 10^4$ cm/s). For these quantities, the characteristic time for attainment of steady state evaporation is of the order of 0.1 μs. If the vapor density is smaller than that assumed in the preceding example, the characteristic collision time increases and the backscattering factor may not achieve its steady state value during the transient. However, when the vapor density is so low that this situation occurs, the collision rate is so small that backscattering can be neglected entirely and β set equal to zero. Conditions for which backscattering of evaporated molecules by the vapor cloud become significant can be calculated by the test-particle method described in Ref. 17. However, situations of practical interest involve strong evaporation in which backscattering is not only significant but occurs rapidly, so that use of the steady state limit (i.e. $\beta = 0.18$) during millisecond-duration transients is justified. Hence the evolution of the temperature and the composition of the condensed phase is independent of the details of the vapor flow away from the surface, and a coupled solid-vapor analysis is not required.

II MATHEMATIC MODEL

II.1 Conservation Equations and Species Fluxes

A condensed phase (solid or liquid) consisting of components A and B occupies the region $x > 0$ which is considered to be semi-infinite in extent. The applicability of this simplification to a particular system depends on the duration of the energy pulse (t_p) and the thickness of the object irradiated. For a material with thermal diffusivity κ, the thermal effect penetrates to a depth of $\sim (\kappa t_p)^{\frac{1}{2}}$. The semi-infinite

medium approximation is valid to the extent that this depth is smaller than the actual thickness. An upper limit to the pulse duration is set at 0.2 ms, which includes most applications to laboratory laser pulsing experiments. With a thermal diffusivity of 0.01 cm^2/s (the value for UO_2), the semi-infinite medium condition is satisfied for specimen thicknesses greater than a few tens of microns.

Because of evaporation at x = 0, the surface recedes with a velocity v. In a coordinate system moving with this surface, the energy balance equation is:

$$\rho \overline{C}_p \left(\frac{\partial T}{\partial t} - v \frac{\partial T}{\partial x} \right) = \frac{\partial}{\partial x} \left(k \frac{\partial T}{\partial x} \right) + Q_v \qquad (2)$$

where T is the temperature, k is the thermal conductivity and $\rho = C_A + C_B$ is the total mass density of the condensed phase. The volumetric heat source Q_v is a prescribed function of time and position. The term $\overline{C}_p$ denotes the effective specific heat of the condensed phase; its use to account for melting is explained in Section II.4. A small term representing the heat transported by the diffusing species has been neglected.

In the same coordinate system, the mass balance on component A is:

$$\frac{\partial C_A}{\partial t} - v \frac{\partial C_A}{\partial x} = - \frac{\partial}{\partial x} j_A \qquad (3)$$

where C_A is the mass concentration of component A in the condensed phase and j_A is its flux. In the moving coordinate system, the condensed phase appears to be flowing in the negative x direction with uniform velocity v, which accounts for the convective term on the left hand side of Eq(3).

Two cases can be distinguished in formulating the diffusive flux of component A in the condensed phase (j_A). For binary solids in which one component is considerably more mobile than the other, the mobile constituent A can be considered to diffuse through a fixed lattice of immobile component B. The diffusive flux is:

$$j_A = - D_A \left(\frac{\partial C_A}{\partial x} + \frac{Q^* C_A}{RT^2} \frac{\partial T}{\partial x} \right) \tag{4}$$

where D_A is the diffusion coefficient of A in the solid, Q^* is the heat of transport and R is the gas constant. The second term on the right hand side of Eq(4) is the Soret flux. Because component B is considered to be immobile, $j_B = 0$, and because it is assumed to form a rigid lattice, the concentration C_B is everywhere constant. In this case there is no conservation equation corresponding to Eq(3) for component B. The composition gradient in the solid is created by vacancies in the sublattice of A. The sublattice of component B remains perfect. This situation is applicable to solid UO_2, where A = oxygen and B = uranium.

The second case of practical importance is applicable to the surface after melting. Since there is no long-range structure in the liquid, diffusion occurs by interchange of A and B atoms in a medium of approximately constant density. The fluxes of A and B relative to the bulk velocity of the liquid are:

$$\begin{aligned} j_A &= - D_{AB} \frac{\partial C_A}{\partial x} \\ j_B &= - D_{AB} \frac{\partial C_B}{\partial x} \end{aligned} \tag{5}$$

where D_{AB} is the mutual diffusion coefficient of the A-B liquid binary(18). Thermal diffusion has been neglected for simplicity. There is a conservation equation for component B comparable to Eq(3), but it provides no

additional information since $C_A + C_B = \rho \simeq$ constant.

II.2 Surface Composition Conditions

The boundary condition for Eq(3) requires matching of species fluxes at x = 0. An observer on the moving boundary sees a flux j_A^g of component A entering the gas phase in the form of one or more molecules containing this element. To balance this loss, condensed phase appears to the observer to flow towards the surface at a velocity v, which provides a flux $vC_A(x = 0)$ of component A. In addition, component A diffuses relative to the bulk condensed phase to produce a negative flux $j_A(x = 0)$. The equality of the fluxes of species A on both sides of the moving boundary is expressed by:

$$j_A^g = \left(-j_A + vC_A\right)_{x=0} \tag{6}$$

A similar flux match applies to component B:

$$j_B^g = \left(-j_B + vC_B\right)_{x=0} \tag{7}$$

Assuming the applicability of the Hertz-Langmiur formula, the vapor fluxes j_A^g and j_B^g are functions only of the surface temperature and a single condensed phase concentration at the surface, such as the A-to-B ratio, C_A/C_B. Assuming that the equilibrium thermodynamics of vaporization indicates vapor phase molecules of the type A_iB_ℓ, the evaporation flux of A is:

$$j_A^g = M_A \sum i\Phi_{A_iB_\ell} \tag{8}$$

where $\Phi_{A_iB_\ell}$ is given by Eq(1) and M_A is the atomic weight of element A. The summation runs over all vapor molecules which contain one or more atoms of A.

The corresponding equation for the vapor flux of component B is:

$$j_B^g = M_B \sum \ell \Phi_{A_i B_\ell} \tag{9}$$

For the case of mobile constituent A in immobile B, the boundary condition at x = 0 is obtained by combining Eqs(4), (6) and (8). Neglecting thermal diffusion, the result is:

$$D_A \left(\frac{\partial C_A}{\partial x} \right)_{x=0} = M_A \sum i \Phi_{A_i B_\ell} - v C_A (x = 0) \tag{10}$$

The recession velocity is obtained by setting $j_B = 0$ in Eq(7) and combining the result with Eq(9):

$$v = \frac{M_B \sum \ell \Phi_{A_i B_\ell}}{C_B} \tag{11}$$

For the liquid surface, the appropriate boundary condition is:

$$D_{AB} \left(\frac{\partial C_A}{\partial x} \right)_{x=0} = M_A \sum i \Phi_{A_i B_\ell} - v C_A (x = 0) \tag{12}$$

The ablation rate of the liquid surface is obtained by adding Eqs(6) and (7) and noting that because $\rho = C_A + C_B \simeq$ constant, $j_A + j_B \simeq 0$:

$$v = \frac{M_A \sum i \Phi_{A_i B_\ell} + M_B \sum \ell \Phi_{A_i B_\ell}}{C_A + C_B} \tag{13}$$

II.3 Surface Heat Fluxes

Radiation incident on an absorbing medium generally decreases in intensity with distance as $e^{-\gamma x}$, where γ is the absorption coefficient

of the material for the radiation. If the pulse duration has a charateristic time t_p, the thermal perturbation penetrates the medium to a distance approximately equal to $(\kappa t_p)^{\frac{1}{2}}$, where κ is the thermal diffusivity. If $\gamma^{-1} \ll \sqrt{\kappa t_p}$, the temperature transient can be satisfactorily represented as driven by a surface heat source. If $\gamma^{-1} \gtrsim \sqrt{\kappa t_p}$, the radiation is best treated by the volumetric heat source term in Eq(2).

In general the rate at which energy enters the condensed phase is smaller than the heat flux arriving at the surface. If the vapor is ionized, optical radiation such as that provided by a laser can be strongly absorbed by the plasma. Even if the vapor is transparent to the incident radiation, a fraction is reflected from the surface and does not contribute to direct heating of the condensed phase. In the case of low energy ion bombardment of a surface, energy is lost by stopping in the vapor even if it consists of neutral species only. This form of vapor shielding of the surface has been treated by Hassanein et al.(19). In the present analysis vapor shielding phenomena are not treated explicitly; instead, the actual energy flux entering the condensed phase is assumed to be specified.

For surface heating, the heat transported by conduction into the condensed phase at x = 0 is the difference between the input due to surface absorption of the incident radiation and heat losses by thermal radiation and to provide the vaporization enthalpy of the emitted molecules. The flux balance is:

$$-k\left(\frac{\partial T}{\partial x}\right)_{x=0} = q_p - q_{rad} - q_{vap} \qquad (14)$$

where q_p is the surface heat source which is assumed to be a pulse of arbitrary temporal shape. The heat lost by thermal radiation, q_{rad}, is usually small compared to the incident flux even at very high temperatures. The heat required to sustain the vapor blowoff is:

$$q_{vap} = \Delta H_v \sum \Phi_{A_i B_\ell} \tag{15}$$

where ΔH_v is the heat of vaporization per mole of component A(or B) and the sum includes all A- (or B-) containing molecules. For example, in applying Eq(13) to UO_2, ΔH_v is the heat of vaporization per mole of UO_2, irrespective of whether the actual evaporating species in U, UO, UO_2 or UO_3. These four vapor species are included in the sum in Eq(13), but terms for the vaporization of O and O_2 are not.

II.4 Treatment of Melting

Transformation from solid to liquid at the melting point introduces a planar heat source which must be taken into account in the thermal analysis. Rather than treat the solid-liquid system as a composite medium requiring a heat balance and temperature equality as matching conditions at the melt boundary, this interface is considered to be a region of nonzero width in which the heat capacity changes rapidly with temperature. This approximation is acceptable because the energy absorbed by melting is usually small compared with that supplied in the pulse. For example, a pulse of 3×10^5 W/cm^2 which lasts for 0.2 ms delivers 60 J per cm^2 of surface. Assume that melting occurs to the depth of penetration of the thermal disturbance, which is $\sqrt{\kappa t_p} \simeq 10^{-3}$ cm for a ceramic such as UO_2 and this surface pulse. For a heat of fusion of 275 J/g and a density of 11 g/cm^3, approximately 3 J/cm^2 are required for melting, which

is $\sim$ 5% of the incident energy density. Surface ablation, on the other hand, has more significant thermal consequences because the heat of vaporization is typically an order of magnitude larger than the heat of fusion.

An apparent heat capacity $\overline{C}_p$ which includes melting can be written as:

$$\overline{C}_p(T) = C_p(T) + \Delta H_f \delta(T - T_f) \tag{16}$$

where C_p is the ordinary specific heat of the condensed phase (solid or liquid depending on the temperature), ΔH_f is the heat of fusion. T_f is the melting point and δ is the Dirac delta function. To avoid the discontinuity at the melting point implicit in Eq(16), which would create difficulties in the numerical solution, the delta function in the last term is replaced by a Gaussian function of half-width ΔT_f. The apparent heat capacity of the condensed phase becomes:

$$\overline{C}_p(T) = C_p(T) + \frac{\Delta H_f}{\sqrt{\pi}\,\Delta T_f} \exp\left[-\left(\frac{T - T_f}{\Delta T_f}\right)^2\right] \tag{17}$$

The enthalpy contained in a layer corresponding to $\pm\sim 2\Delta T_f$ of melting point, which is the integral of $\overline{C}_p(T)$, is the same when calculated from Eq(16) or Eq(17). Computed temperature distributions are not sensitive to the choice of the temperature range over which fusion is artificially spread. The value ΔT_f = 50 K has been used in all calculations.

All other physical properties can change discontinuously at the melting point without creating computational difficulties. Dependence of properties on composition is ignored for lack of information, particularly in the liquid state.

II.5 Other Conditions

Conditions prior to the transient and far from the surface need to be specified. These are:

$$\left.\begin{array}{l} T = T_o \\ \\ C_A = C_{Ao} \end{array}\right\} \text{for} \quad \begin{array}{l} t = 0, \text{ all } z \\ \\ z = \infty, \text{ all } t \end{array} \tag{18}$$

In some applications, the solid irradiated by the pulse may initially support a nonuniform temperature distribution instead of the uniform temperature specified in Eq.(18). The temperature transient produced by the energy pulse at the surface can simply be added to the pre-existing distribution provided that the latter would not have changed significantly during the duration of the pulse due to cooling mechanisms acting on the unirradiated surfaces. If such cooling is important, the linearity of heat conduction permits the problem of relaxation of the initial temperature distribution to be treated independently of the calculation of the temperature transient induced by the energy pulse on the surface(20). Although the high temperatures and surface ablation involved in the thermal response to the pulse introduce nonlinearities into the heat transfer process, these are not strongly coupled to the computation of the change in an initial distribution during the pulse, and separability of the two thermal problems remains an acceptable simplification.

III NUMERICAL SOLUTION METHOD

Nonlinearities resulting from the temperature-dependent thermal properties, the convective-like term appearing from coordinate transformation, the moving melting front and the boundary conditions containing the strongly temperature-dependent ablative term, make analytical solution impossible. In addition, for an incongruently vaporizing binary materials, the heat and mass transport equations are strongly coupled. The linkage occurs because the vaporization fluxes defined by Eq(1) depend upon the

temperature and the composition at the surface. These fluxes determine the recession velocity by Eqs(11) or (13), which appears in the conservation equations given by Eqs(2) and (3). The vaporization fluxes also appear in the surface energy balance via Eqs(14) and (15). A consequence of this coupling is that the surface temperature excursion is dependent upon the diffusion coefficient of component A in the condensed phase.

Numerical solution is accomplished by the Crank-Nicolson finite difference method, in which the space and time derivatives are replaced by second order correct finite difference representations. The Newton-Raphson method is used to carry out the iterations. Although this combination of numerical techniques is not very efficient for highly nonlinear problems, it works quite well for a smoothly-varying heat source with a predictor-corrector scheme for constructing good initial guesses for iterations. Gaussian elimination back-substitution is an efficient way to solve the resulting system of linear equations. Furthermore instead of using constant space and time increments, as usually done for slowly-varying problems, the space increment is varied in a geometrical manner and the time variation is determined by multistep method. Details of the numerical analysis are given in Ref. 21.

IV. RESULTS

This section presents calculated temperature and composition variations in initially stoichiometric UO_2 which is subjected to high intensity laser irradiation. The laser pulse is roughly triangular in shape and lasts approximately 400 μs. The energy contained in the pulse varies from 10 to 30 J which, for an illuminated spot of 0.5 cm^2, produces peak

power densities ranging from 1×10^5 to 3×10^5 W/cm^2. The equations presented in Section II are used in the computation. Bulk heating (Q_v in Eq(2)) is neglected because polycrystalline UO_2 above $\sim$ 1700 K is opaque to the incident radiation. Thermal diffusion by the Soret effect is negligible. It makes little difference if the recession velocity is computed by Eq(11) or by Eq(13); the mobile constituent (A = oxygen) is so light compared to uranium that these two expressions for v are essentially equivalent. The approximate treatment of subsurface melting described in Section II.4 is used in this analysis. The temperature-dependent physical properties of UO_2 needed for the analysis are given in Ref. 21. Using the best estimates of these properties and an initial temperature of 1600 K, the changes in surface temperature and surface O/U ratio for a 10 J pulse are shown in Fig. 1. The surface temperature reaches a maximum of 3950 K slightly after the peak of the laser pulse and decreases slowly thereafter. The surface O/U ratio attains a minimum value of 1.95 at about the same time that the temperature peaks. The solid becomes depleted of oxygen due to preferential vaporization of UO_3 from the liquid. However, a recovery of the surface oxygen concentration occurs late in the transient due to oxygen diffusion from the stoichiometric bulk solid. For an incident laser pulse of 30 J, a maximum surface temperature of 4610 K and a minimum O/U ratio of 1.75 are reached. For steady temperatures equal to the maxima achieved in the 10 and 30 J pulses, Breitung's forced congruent vaporization model(8) predicts surface O/U ratios of 1.89 and 1.57, respectively. These oxygen depletions are more severe than those using the present full transient analysis. The oxygen-depleted layer extends to a depth of $\sim$ 6 μm below the surface.

The calculations which produced the results shown in Fig. 1 assume a perfectly defined set of input values, each combination of which produces a unique output response (i.e., surface temperature or surface composition). However, many of the input variables can only be specified within a range of likely values, and as a result of this imprecision, the plots shown in Fig. 1 should be bands rather than lines. The "response surface method" developed in Refs 22 and 23 for application to fuel modeling codes provides a quantitative means of calculating the fuzziness of the output caused by uncertainties in the input variables. Application of this method to the calculation outlined in the preceding sections is presented in quantitative detail in Ref. 17, and only a qualitative description of the technique is given here.

For example, the thermal conductivity of liquid UO_2 is judged to fall in a range bracketed by 0.044 and 0.031 W/cm-K, the heat of vaporization to be between 980 and 1960 J/g, and the oxygen diffusivity to follow either of the following formulas:

$$D_O = \begin{cases} 0.016e^{-2620/T} \\ \quad \text{or} \\ 0.3e^{-24800/T} \end{cases} \qquad (cm^2/s)$$

A "response surface" is a representation of the maximum surface temperature, for example, as a function of the three variables specified as uncertain within the ranges given above. The response surface can be characterized by a mean value and by a variance, the latter depending on the uncertainties in all of the input variables. In addition, the fractional contributions of each variable to the total uncertainty in the output can be determined by the response surface

method. The results of the sensitivity analysis on the behavior of UO_2 in a laser pulse over a range of laser energies are shown in Fig. 2. The solid lines represent the mean (or best estimate) output quantities and the dashed lines indicate the variance due to uncertainties in the input data. The uncertainty in the predicted maximum surface temperature is approximately ± 150 K, and that of the composition nearly a tenth of an O/U unit. As expected, the uncertainty in the thermal conductivity and heat of vaporization have the greatest effect on the thermal response. However, for the 30 J pulse, the lack of precise knowledge of the oxygen diffusion coefficient adds more to the variance of the surface temperature maximum than does uncertainty in the thermal conductivity.

V. CONCLUSIONS

A mathematical model and numerical scheme have been developed to simulate the temperature excursion and component redistribution of a solid subjected to a high power energy pulse. Application of the computational method to the response of uranium dioxide to laser pulses illustrated the importance of correctly accounting for component redistribution driven by the composition changes induced by incongruent vaporization. The response surface method was used for the sensitivity analyses of the effect of uncertainties of some of the material properties of UO_2 on the response of the system to transient pulsing.

ACKNOWLEDGEMENT

This work has been supported by the Director, Office of Energy Research, Office of Basic Energy Science, Materials Science Division of the U.S. Department of Energy under contract No. DE-AC03-76SF00098.

REFERENCES

1. N. Asami, M. Michikawa and M. Tagnchi, IAEA Symp. on Thermodynamics of Nuclear Materials, Paper IAEA-SM-190/3, Vienna Oct. 1974.
2. R. W. Ohse, P. G. Barrie, H. G. Bogensberger and E. A. Fischer, IAEA Symp. on Thermodynamics of Nuclear Materials, Paper IAEA-SM-190/8, Vienna Oct. 1974.
3. M. Bober, H. U. Karow and K. Schretzmann, IAEA Symp. on Thermodynamics of Nuclear Materials, Paper IAEA-SM-190/34, Vienna Oct. 1974.
4. W. Breitung, "Vapor Pressures of Oxide Reactor Fuels above 3000 K: Review and Perspective", NUREG/CR-2261(1981).
5. R. W. Ohse, P. G. Barrie, H. G. Bogensberger and E. A. Fischer, J. Nucl. Mater. 59 (1976) 112.
6. F. W. Dabby and U-C Paek, IEEE J. Quan. Elec. Vol. QE-8, No. 2, Feb. 1972.
7. H. U. Karow and M. Bober, IAEA Symp. on Thermodynamics of Nuclear Materials, Paper IAEA-SM-236/22, Julich, Jan. 1979.
8. W. Breitung, "Evaporation Kinetics of Oxide Fuels and their Consequences on Actinide Redistribution in Reactor Fuel Pins and Fuel Vapor Pressures under conditions of Core Disruptive Accidents", Kernforschungszentrum Karlsruhe Report KfK-2240, June, 1976.
9. R. A. Olstad and D. R. Olander, J. Appl. Phys. 46 (1975) 1509
10. G. A. Somorjai and J. E. Lester, Progr. Solid State Chem. IV (1967) 1.
11. G. M. Pound, J. Phys. & Chem. Ref. Data, 1 (1972) 135.
12. S. I. Anisimov, Soviet Phys. JETP, 27 (1968) 182.
13. T. Ytrehus, Tenth Inter. Symp. on Rarefied Gas Dynamics, 51 (1976) 1197.

14. B. J. Merrill, INTOR Report INTOR/NUC/81-7 (1981).

15. R. W. Schrage, "A Theoretical Study of Interphase Mass Transfer", Columbia Univ. Press, New York (1953).

16. S. I. Anisimov and A. K. Rakhmatulina, Sov. Phys. JETP 37 (1973) 441.

17. C. H. Tsai, "The Kinetics of Laser Pulse Vaporization of UO_2 by Mass Spectrometry", PhD Thesis, University of California, Berkeley, LBL-13679, Nov. 1981.

18. R. B. Bird, W. E. Stewart and E. N. Lightfoot, "Transport Phenomena", Wiley (1960).

19. A. M. Hassanein, G. L. Kulcinski and W. G. Wolfer, J. Nucl. Mater. 103/104 (1981) 321.

20. H. S. Carslaw and J. C. Jaeger, Conduction of Heat in Solids, Oxford University Press, London and N. Y. 1967.

21. C. H. Tsai, "Numerical Simulation of Transient Incongruent Vaporization Induced by High Power Lasers" LBL-12125 (1981).

22. N. D. Cox, "A Report on a Sensitivity Study of the Response Surface Method of Uncertainty Analysis of a PWR Model," EG&G Idaho, Inc., Report No. RE-S-77-7, January 1977.

23. S. O. Peck, "Code Development and Analysis Program", EG&G Idaho, Inc. Report No. CDAP-TR-78-024, July 1978.

LIST OF FIGURES

1. (a) Surface temperature transient and (b) the surface composition transient for a 10 J laser pulse on UO_2. The peak of the pulse occurs after 50 μs from the start of irradiation and the pulse terminates after 400 μs.

2. (a) Mean and variance of the maximum surface temperature and (b) the surface composition at the time of the maximum surface temperature. The slope discontinuity in the temperature plot is due to a change in the temporal shape of the laser pulse which occurs at ~ 11 J. The uncertainties are represented by the zone bounded by the dashed lines.

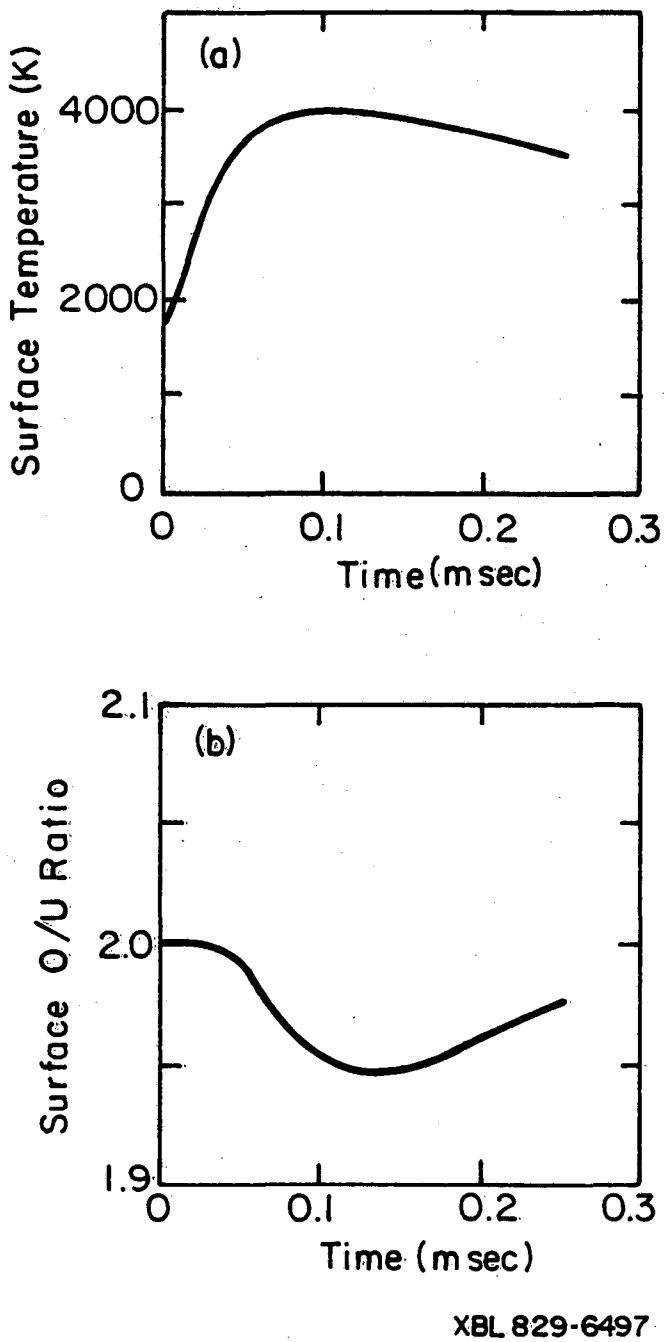
(a)
Surface Temperature (K)
4000
2000
0
0
0.1
0.2
0.3
Time (m sec)
(b)
Surface O/U Ratio
2.1
2.0
1.9
0
0.1
0.2
0.3
Time (m sec)
XBL 829-6497

Figure 1.

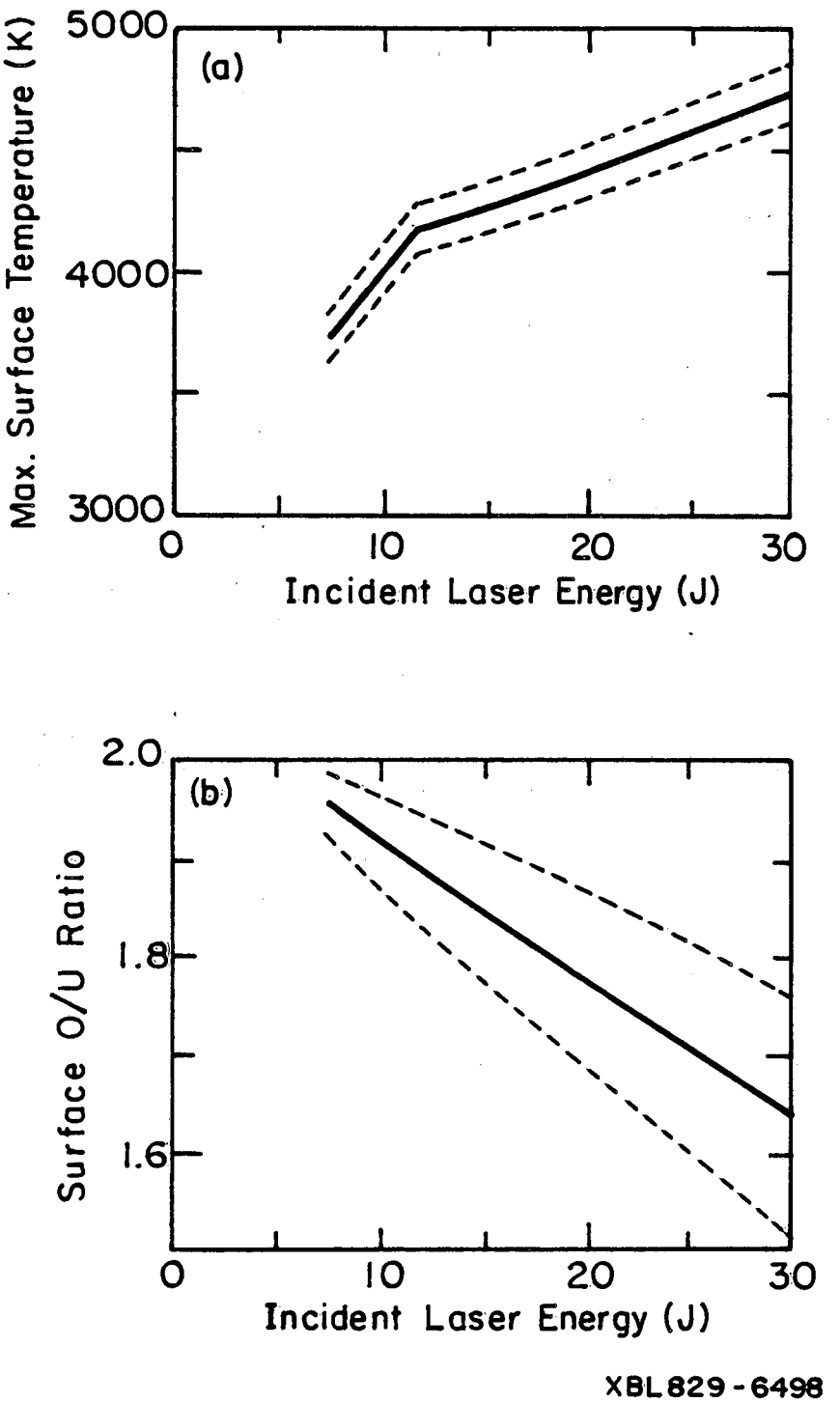
(a)
Max. Surface Temperature (K)
5000
4000
3000
0
10
20
30
Incident Laser Energy (J)
(b)
Surface O/U Ratio
2.0
1.8
1.6
0
10
20
30
Incident Laser Energy (J)
XBL829-6498

Figure 2.

This report was done with support from the Department of Energy. Any conclusions or opinions expressed in this report represent solely those of the author(s) and not necessarily those of The Regents of the University of California, the Lawrence Berkeley Laboratory or the Department of Energy.

Reference to a company or product name does not imply approval or recommendation of the product by the University of California or the U.S. Department of Energy to the exclusion of others that may be suitable.

TECHNICAL INFORMATION DEPARTMENT
LAWRENCE BERKELEY LABORATORY
UNIVERSITY OF CALIFORNIA
BERKELEY, CALIFORNIA 94720